Available online at www.sciencedirect.com
ScienceDirect
Earth and Planetary Science Letters 254 (2007) 55–68
EPSL
www.elsevier.com/locate/epsl

Lu–Hf, in-situ Sr and Pb isotope and trace element systematics for mantle eclogites from the Diavik diamond mine: Evidence for Paleoproterozoic subduction beneath the Slave craton, Canada

Stefanie S. Schmidberger [a,*], Antonio Simonetti [a], Larry M. Heaman [a], Robert A. Creaser [a], Sean Whiteford [b]

[a] *Earth and Atmospheric Sciences, University of Alberta, Edmonton, AB, Canada T6G 2E3*
[b] *Diavik Diamond Mines, Yellowknife, NWT, Canada*

Received 19 December 2005; received in revised form 10 November 2006; accepted 10 November 2006
Available online 22 December 2006
Editor: R.D. van der Hilst

Abstract

Lu–Hf, Sm–Nd and in-situ clinopyroxene Sr and Pb isotope systematics, and mineral major and in-situ trace element compositions were obtained for a suite of non-diamond and diamond-bearing eclogites from the Diavik kimberlites (A154; 55 Ma old), Slave craton (Canada). Temperature estimates of last equilibration in the lithosphere for the non-diamond-bearing Diavik eclogites define two groups; low-temperature (800–1050 °C) and high-temperature eclogites (1100–1300 °C). Most diamond–eclogites indicate temperatures similar to those of the high-temperature eclogites. Isotopic and major and trace element systematics for the non-diamond- and diamond-bearing eclogites indicate overlapping chemical compositions suggesting similar rock formational histories. Calculated whole rock major and trace element abundances using chemical and modal abundances for constituent minerals exhibit broad similarities with mafic cumulates from ophiolite sequences. Most importantly the calculated whole rock eclogite compositions display positive Sr and Eu anomalies, typically interpreted as the result of plagioclase accumulation in cumulate rocks of oceanic crust sequences. Initial whole rock Hf isotopic values and in-situ Sr isotope data from clinopyroxene grains provide evidence that the eclogites were derived from precursor rocks with depleted mantle isotope characteristics. These combined results support the interpretation that the eclogites from Diavik represent remnants of subducted oceanic crust. Lu–Hf isotope systematics indicate that the oceanic protolith for the eclogites formed in the Paleoproterozoic at ~2.1 Ga, which is in agreement with the in-situ Pb isotope data from clinopyroxene. This result also corroborates the ~2.1 Ga Lu–Hf model ages recorded by mantle zircons from eclogite found within the Jericho kimberlite in the northern Slave Province (~200 km northwest of Diavik). The results from both studies indicate a link between eclogite formation and Paleoproterozoic subduction of oceanic lithosphere along the present-day western margin of the Archean Slave craton.

Keywords: eclogite; subduction; Slave craton; isotopes; trace elements; laser ablation analysis

1. Introduction

Subcontinental lithosphere is mainly composed of refractory peridotite but also contains a small but

* Corresponding author. Tel.: +1 780 492 4354.
E-mail address: stefanie.schmidberger@ualberta.ca (S.S. Schmidberger).

0012-821X/$ - see front matter © 2006 Elsevier B.V. All rights reserved.
doi:10.1016/j.epsl.2006.11.020

petrologically important amount of eclogites. Mantle eclogites are found in many kimberlites (e.g. [1,2]) and their study provides invaluable insights into the geochemical and isotopic composition, and formational history of cratonic mantle roots. Of great economic interest, mantle eclogites are an important source of diamond, and eclogitic diamond populations dominate a number of world-class diamond deposits (e.g. [3]). The origin of eclogites is still a matter of debate with several different formational models being advocated. These include eclogite formation via magmatic processes resulting from fractionation of basic magmas at high pressure in the Earth's mantle (e.g. [4]) or subduction of oceanic lithosphere (e.g. [5]), which can include the transformation of low-pressure mafic cumulates, such as gabbros, into eclogite (e.g. [6]). Several previous stable and radiogenic isotope and trace element investigations indicate that many eclogite xenoliths are products of high-pressure metamorphism of altered ocean-floor rocks that have been added to the cratonic lithosphere via subduction and slab subcretion (e.g. [1]). However, the timing of eclogite formation is currently poorly constrained. The effects of element diffusion and isotope exchange at lithospheric temperatures and pressures (e.g. [7,8]), and repeated episodes of mantle metasomatism that perturb most isotope chronometers (e.g. Sm–Nd, Rb–Sr; [9,10]) have proven age determinations of mantle-derived rocks difficult. However, recent studies have demonstrated the relatively robust nature of the Lu–Hf chronometer, resisting chemical changes imposed on mantle-derived rocks as the result of interaction with metasomatic melts or fluids in the Earth's mantle (e.g. [11,12]).

Geochemical and isotopic studies of the lithospheric mantle beneath cratons in Canada remain sparse because until recently these regions have been relatively inaccessible to direct investigation. Within the last few years, the discovery of diamondiferous kimberlites in Canada and their extensive exploration in the Northwest Territories have opened access to unique mantle samples from the deep cratonic lithosphere. Many of the newly discovered kimberlites contain eclogite xenoliths (e.g. [13]), a number of which are diamond-bearing, that are suitable for geochemical studies because of their relatively fresh nature and fairly large sample size. These investigations have begun to unravel the age, formation and evolution of the subcratonic mantle beneath Canada (e.g. [12,14]). Our investigation focuses on a suite of kimberlite-hosted mantle eclogites and diamond-bearing mantle eclogites from the Diavik diamond mine (Slave Province, NWT). We report Lu–Hf, Sm–Nd and in-situ clinopyroxene Sr and Pb isotope data and mineral major and in-situ trace element compositions for eclogites and diamond-bearing eclogites obtained by laser ablation-ICP-MS and MC-ICP-MS (multicollector inductively coupled plasma mass spectrometry) analysis. The results presented here provide important information on the origin and age of the Diavik mantle eclogites. These findings also help unravel the tectonic development of the Archean Slave craton and support the presence of remnants of Paleoproterozoic oceanic fragments in the cratonic lithosphere.

2. Geology and samples

The Slave Province is a relatively small Archean craton (~700×500 km) that forms part of the Canadian Shield and is bounded by Paleoproterozoic orogenic belts to the west (1.9–1.8 Ga Wopmay orogen) and to the east and southeast (2.0–1.9 Ga Taltson–Thelon orogen) (e.g. [15–17]). The craton is composed of Mesoarchean basement (4.0–2.9 Ga) in the western and central parts, and Late Archean isotopically juvenile rocks (<2.85 Ga) in the east [18]. The diamondiferous Diavik kimberlites are located just off shore a 20 km^2 island (East Island) within the Lac de Gras area in the central Slave Province (Latitude: 64° 30′ 41″, Longitude: 110° 17′ 23″) ~300 km northeast of Yellowknife (Fig. 1). The kimberlites (total of 53 pipes) were emplaced 55 Ma ago into Archean granitic and metasedimentary rocks of the Contwoyto terrane [19]. The Diavik mine has been in operation since January 2003 with diamonds being mined from kimberlite pipes A154 South and A154 North. The Diavik pipes are small (0.9–1.6 ha) compared to the world average (12 ha), but contain a higher than average content of high-quality diamonds. The estimated reserves of the Diavik diamond deposits are 29.8 million tonnes at an average of 3.2 ct/tonne with an annual diamond production peaking at 8 million carats.

The Diavik kimberlites host abundant mantle xenoliths including an unusually well-preserved suite of mantle-derived eclogites. The eclogite xenoliths analyzed in this study (n=46) were sampled from pipes A154 South and A154 North during open pit mining operation. The mantle xenolith suite also contains diamond-bearing eclogites, and those investigated here were recovered from the Diamond Splitting Facility (n=8). The xenolith suite is subdivided into two groups and referred to as 'eclogites' and 'diamond–eclogites'. Both groups are characterized by bimineralic compositions consisting of pyrope–almandine-rich garnet and omphacitic clinopyroxene. Accessory mineral phases

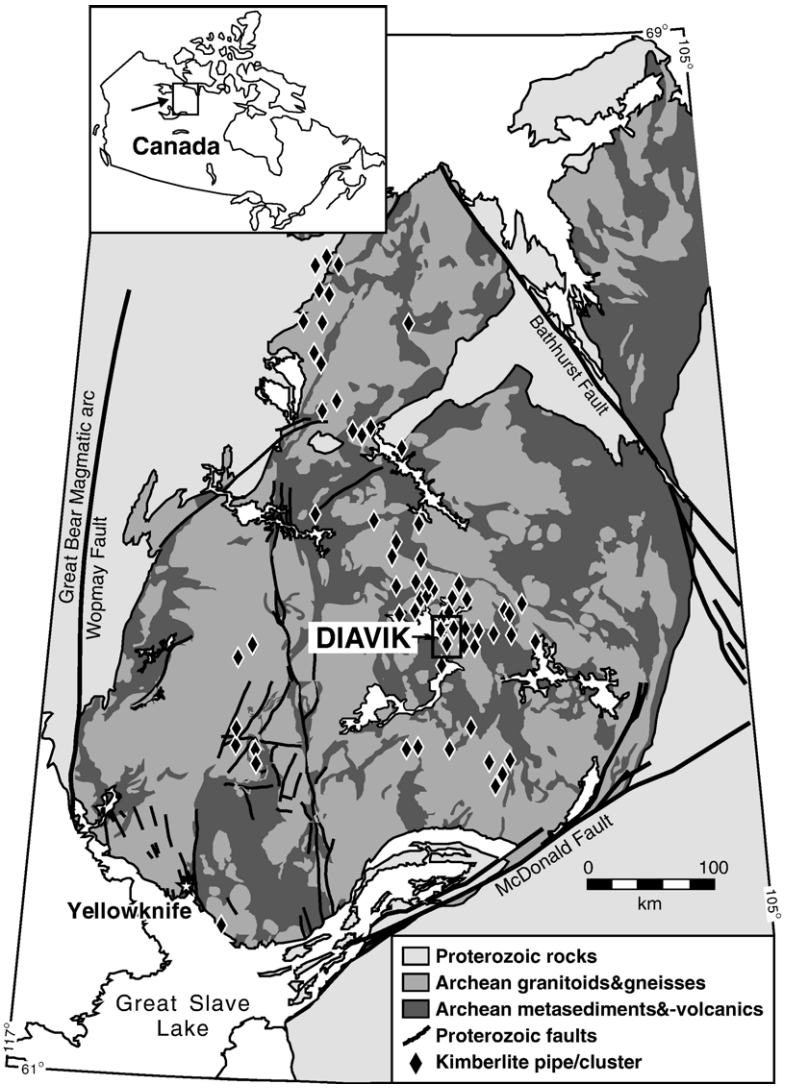

Fig. 1. Geological map of the Slave Province showing kimberlite locations.

include rutile, phlogopite, iron oxides and sulfides. Modal amounts of constituent garnet and clinopyroxene range between 70–35% and 65–30% (online data), respectively. The majority of the eclogites and diamond–eclogites are coarse-grained (~75%) with a smaller number of samples exhibiting fine-grained textures (~25%). Most xenoliths are characterized by primary granoblastic microstructures.

3. Analytical methods

The whole rock eclogites were crushed with a hammer between thick plastic sheets and rock chips free of alteration rims were ground in an agate mill. Garnet and clinopyroxene separates were hand-picked under a binocular microscope and inclusion free grains were washed in an ultrasonic bath with acetone, ultra pure water and 2.5 N HCl. Mineral separates for solution mode isotope analysis were crushed in an agate mill. Crushed kimberlite whole rocks were carefully hand-picked under a binocular microscope prior to grinding in an attempt to eliminate contamination from xenocrysts and country rock fragments. Inclusion-free clinopyroxene grains were embedded into epoxy mounts for laser ablation analyses and surfaces were polished to 0.3 μm.

Chemical separation of Hf and Lu for whole rock eclogites, constituent minerals and kimberlite follows the procedure described in Bizzarro et al. [20]; protocol for solution mode MC-ICP-MS analysis is outlined in Schmidberger et al. [11]. REE fractions were collected

during the chemical separation of Hf and Lu [20] and the analytical procedure for the purification of Nd and Sm follows the technique described by Creaser et al. [21]. Solution mode Lu–Hf and Sm–Nd isotope analyses were performed on a NuPlasma MC-ICP-MS at the University of Alberta Radiogenic Isotope Facility. Repeated measurements ($n=47$) of a 50 ppb solution of the JMC 475 Hf isotopic standard yield the following average values: $^{176}Hf/^{177}Hf=0.282158\pm16$, $^{178}Hf/^{177}Hf=1.46727\pm7$, $^{180}Hf/^{177}Hf=1.88676\pm21$ (2σ standard deviation). Repeated analysis of a 200 ppb solution of the in-house Alpha Nd isotopic standard ($n=256$) yields: $^{143}Nd/^{144}Nd=0.512240\pm20$.

Laser ablation isotopic analyses were obtained using an Nd:YAG UP213 nm laser system (New Wave Research) coupled to the NuPlasma MC-ICP-MS at the University of Alberta Radiogenic Isotope Facility. The analytical protocol for in-situ Sr isotope analyses follows the method outlined in Schmidberger et al. [22]. Clinopyroxenes were ablated in a Helium atmosphere (1.0 L/min) using the following parameters: 60 s ablation time; 160 μm spot size; 20 Hz repetition rate; ~15 J/cm^2 energy density. In-situ Pb isotope analyses were obtained using the identical laser ablation parameters as those described for the in-situ Sr isotope analyses. The sample-out line from the laser ablation cell was 'y'-connected to the sample-out line from the desolvating nebulizing introduction system (DSN-100 from Nu Instruments) to allow for simultaneous aspiration of a dilute Tl solution. The latter was used to monitor and correct for instrumental mass bias of the measured Pb isotope ratios, similar to the procedure described by Simonetti et al. [23]. The Pb and Tl isotope ion signals were measured simultaneously using six Faraday collectors. The accuracy of the analytical protocol was evaluated with repeated analysis ($n=10$) of an amazonite feldspar in-house standard from the Broken Hill deposit, Australia. The average Pb isotope values obtained here (Table 4) are indistinguishable from those previously obtained by TIMS measurement for the ore from the Broken Hill deposit [24].

In-situ trace element analyses of individual clinopyroxene and garnet grains were obtained using an ELAN6000 quadrupole ICP-MS coupled to a UP213 nm laser ablation system at the University of Alberta. The optimization of ICP-MS instrument parameters (RF power 1200 W, peak hopping acquisition, 50 ms dwell time) was achieved by ablating the NIST 612 glass standard. For trace element determinations, the NIST 612 standard, clinopyroxene, and garnet grains were ablated using a 160 μm spot size, 5 Hz repetition rate and energy density of ~13 J/cm^2. Ablation runs were conducted in a mixed He/Ar atmosphere (ratio of 0.5:0.1 L/min), and mixed with Ar (1.03 L/min) prior to entering the torch assembly. The laser ablation cell was flushed with a higher flow rate of He (up to 0.9 L/min) for approximately 1 min in-between laser ablation runs to ensure adequate particle wash-out. A typical analysis consisted of a ~25 s background measurement followed by ablation for ~40 s. The NIST 612 glass standard was used as the external calibration standard. Quantitative results for 23 elements (Table 1) were obtained via the calibration of relative element sensitivities using the NIST 612 standard, and normalization of each analysis to the electron microprobe data for Ca as the internal standard. Data reduction and concentration determinations were obtained using the GLITTER® (XP version, Macquarie University) laser ablation software. Repeated analysis ($n=13$) of the NIST 612 glass as an unknown over the period of two days yields relative standard deviations of between 2 to 9% (2σ level; Table 1) for the elements investigated here. The average concentration values obtained for the 'unknown' NIST 612 glass standard analyses deviate <1% compared to the accepted values for the elements reported in Table 1, with the exception of Pb (4% deviation). The accuracy of the trace element concentrations determined here for garnet was evaluated by repeated analysis of the PN2 garnet standard. The latter has been analyzed using various analytical techniques (INAA, SIMS, LA-ICP-MS) from several laboratories world-wide [25]. The average concentration values obtained here for the PN2 garnet (Table 1) overlap and are in agreement with the range of values reported in Canil et al. [25]. The relative standard deviation (2σ) for most elements measured in the garnet grains investigated here ranges from 3 to 15% (Table 1). Detection limits for most trace elements vary between 0.01 and 0.05 ppm. Major element compositions for constituent eclogite minerals were determined using electron microprobe analysis at the University of Alberta (for analytical parameters see online data table).

4. Results

4.1. Mineral compositions

The eclogite garnets are pyrope–almandines and show a large variation in MgO (6.1–20.4 wt.%), CaO (2.9–13.8 wt.%) and FeO (8.4–20.0 wt.%) contents (online data; Fig. 2A). Magnesium numbers (Mg/(Mg+Fe) for the eclogite garnets vary from 0.33 to 0.81. The diamond–eclogite garnets are also pyrope–almandine-rich and characterized by less variable MgO (6.3–13.3 wt.%), CaO (7.6–14.6 wt.%) and FeO (11.4–

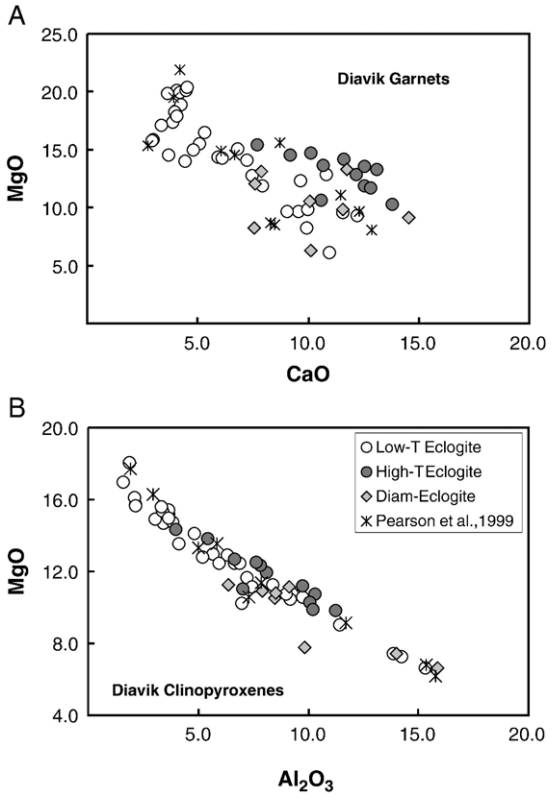

Fig. 2. Major element variation diagrams for (A) garnets and (B) clinopyroxenes from Diavik eclogites and diamond–eclogites. Data for other Diavik eclogite garnets and clinopyroxenes are shown for comparison [26].

23.1 wt.%) contents compared to the eclogites (online data; Fig. 2A). Diamond–eclogite garnets have magnesium numbers of 0.33 to 0.68. Garnets from eclogites and diamond–eclogites do not exhibit chemical zoning and are homogeneous at the thin section scale. Mineral chemical data for diamond–eclogites overlap those for the eclogites, but do not extend to high MgO-low CaO compositions as observed for the latter (Fig. 2A). Previously reported major element data (e.g. MgO; CaO) for eclogitic garnets from Diavik [26] overlap entirely with those for the eclogite garnets investigated here (Fig. 2A).

The eclogite clinopyroxenes are omphacites with Na_2O contents ranging from 1.1 to 8.7 wt.% (online data). Na_2O contents for the diamond–eclogite clinopyroxenes are less variable (4.0 to 7.0 wt.%; online data). Magnesium numbers for clinopyroxenes from the eclogite (0.77–0.94) trend to slightly higher values compared to those for clinopyroxenes from the diamond–eclogite (0.64–0.86). All clinopyroxenes are characterized by a homogeneous mineral chemistry as observed for the eclogite garnets. Al_2O_3 contents are positively correlated with Na_2O, and negatively correlated with MgO abundances in clinopyroxenes from eclogite and diamond–eclogite. Compositional data for both groups overlap those previously reported eclogitic clinopyroxenes from Diavik ([26]; Fig. 2B).

4.2. Temperature estimates

Temperatures of last equilibration in the lithosphere were calculated using a garnet–clinopyroxene Fe–Mg exchange geothermometer [27]. The calculated temperatures for the eclogites range from 770 °C to 1325 °C (online data; Fig. 3) when calculated at a nominal pressure of 50 kb. These temperatures are similar to those calculated for previously reported data from Diavik eclogites (880 °C–1250 °C; $n=9$) when using the same geothermometer [26,27]. The diamond–eclogites exhibit less variable and overall higher temperatures varying between 1127 °C and 1299 °C (except sample 20705E1; 860 °C). In contrast, the eclogites define a bimodal temperature distribution-low-temperature (<1100 °C) and high-temperature (>1100 °C) groups (Fig. 3). Mineral chemical data for garnet and clinopyroxene from both low-temperature and high-temperature eclogites overlap, while garnets in the high-temperature eclogites plot on the high CaO (7.7–13.8 wt.%) and low MgO (10.3–15.4 wt.%) and FeO (8.4–15.9 wt.%) side of the garnet compositional array (online data).

4.3. Trace element compositions

Incompatible trace element and rare earth element (REE) contents were determined for garnets and clinopyroxenes from six low-temperature and three

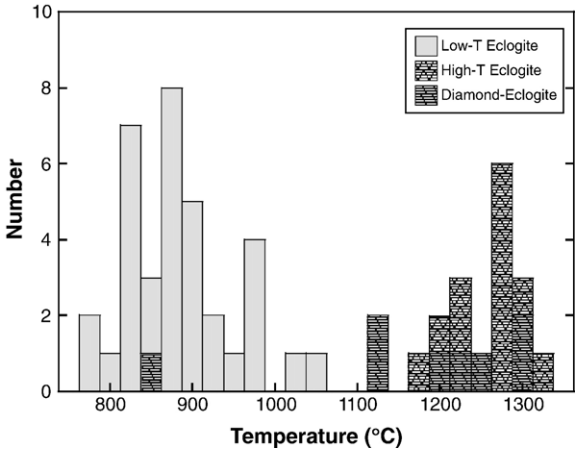

Fig. 3. Temperature estimates for Diavik eclogites and diamond–eclogites [27]. Data for eclogites show a bimodal temperature distribution suggesting classification in low-temperature (<1100 °C) and high-temperature (>1100 °C) eclogites.

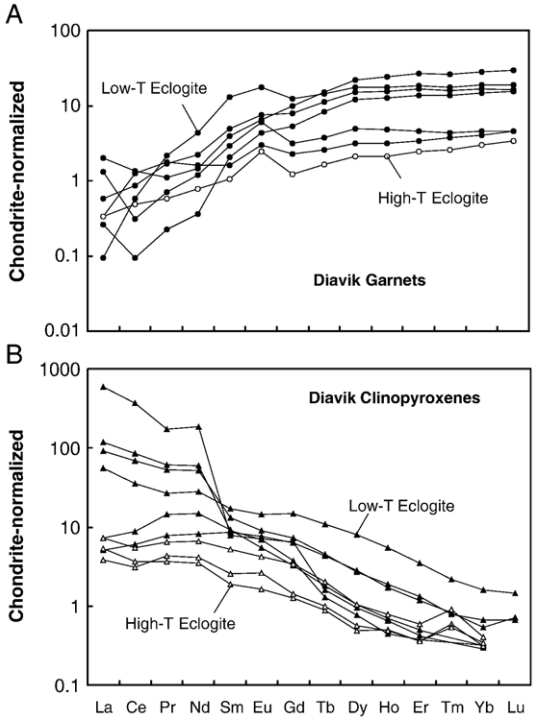

Fig. 4. Chondrite-normalized rare earth element patterns for (A) garnets and (B) clinopyroxenes from low-temperature and high-temperature Diavik eclogites [28].

high-temperature eclogites. The garnets are characterized by an enrichment in heavy rare earth elements (HREE; e.g. Lu, 3–30 times chondrite; [28]) compared to their light rare earth element (LREE) abundances (Table 1; Fig. 4A). The majority of the LREE patterns are not steeply dipping, but show concave-upward trends in a chondrite-normalized plot (Fig. 4A). Of importance, all garnets (except MX-3) exhibit positive Eu anomalies (Eu/Eu* = 1.2 to 2.2; Table 1). Abundances of highly incompatible trace elements in the garnets are low (e.g. Rb, Ba; Table 1). The incompatible trace element patterns for the high-temperature garnets are indistinguishable from those for the low-temperature eclogite garnets. Clinopyroxenes are characterized by an enrichment in the LREE (e.g. La, 4–600 times chondrite) compared to HREE abundances (Table 1; Fig. 4B). LREE abundances in a number of clinopyroxenes (e.g. La, 60–600 times chondrite; MX2, MX3, MX7, MX15) are significantly higher compared to those of the remaining samples (e.g. La, 4–7 times chondrite; Fig. 4B). Small positive Eu anomalies can be observed for half of the clinopyroxene samples (Eu/Eu* = 1.1 to 1.3; Table 1). Most highly incompatible trace element abundances are low compared to those for the LREEs (Table 1). High-temperature eclogite clinopyroxenes have incompatible trace element patterns that are similar to those for clinopyroxenes from the low-temperature eclogites but the former are characterized by overall lower elemental abundances (Table 1).

4.4. Lu–Hf and Sm–Nd isotope data

4.4.1. Kimberlite

Two Diavik kimberlite samples were collected from pipe A154 South and initial Hf and Nd isotopic compositions were calculated using an emplacement age of 55 Ma. The kimberlite is characterized by low $^{176}Lu/^{177}Hf$ ratios (0.008; 0.009) and has essentially chondritic initial $^{176}Hf/^{177}Hf_{(55\ Ma)}$ (0.282706; 0.282716; [29]), corresponding to initial $\varepsilon_{Hf(55\ Ma)}$ values of −1.1 and −0.8 (Table 2; Fig. 5A). $^{147}Sm/^{144}Nd$ ratios (0.067) for the kimberlite are subchondritic and $^{143}Nd/^{144}Nd_{(55\ Ma)}$ ratios (0.512403; $\varepsilon_{Nd(55\ Ma)}$ values of −3.2; Table 2; Fig. 5A) that are slightly enriched compared to CHUR (chondrite uniform reservoir).

Previous studies have subdivided South African kimberlites into “Group I” and “Group II” based on their distinct mineralogy and isotopic signatures, indicating

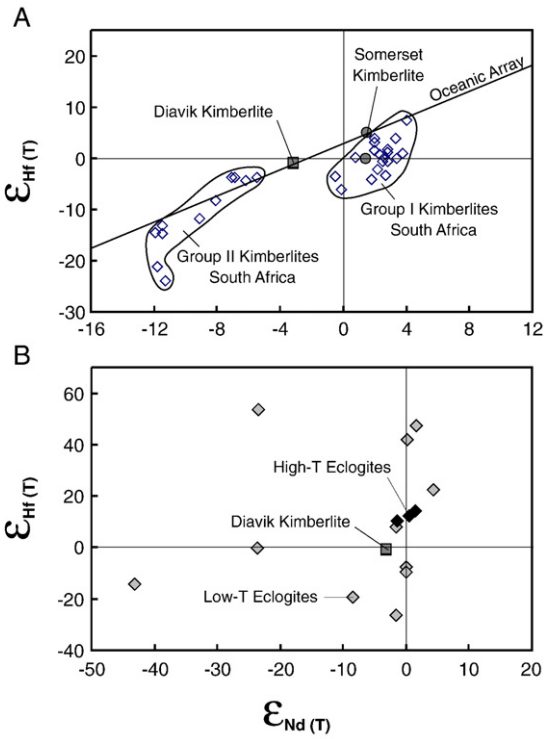

Fig. 5. Hf–Nd variation diagram for (A) Diavik kimberlite showing initial isotopic compositions (at 55 Ma) and (B) Diavik eclogites at the time of kimberlite emplacement. Also shown in (A) are initial isotope ratios for South African “Group I” and “Group II” kimberlites and Somerset Island kimberlites, Canadian Arctic [8,11,32]. The oceanic array defined as $\varepsilon_{Hf} = 1.33\ \varepsilon_{Nd} + 3.19$ is plotted for comparison [33].

derivation from isotopically distinct mantle domains [30,31]. The Diavik kimberlite has initial $^{176}Hf/^{177}Hf$ ratios that overlap the range defined by the South African "Group I" kimberlites, while their $^{143}Nd/^{144}Nd$ are less radiogenic ([32]; Fig. 5A). In an Nd and Hf isotope diagram, initial ratios for the Diavik kimberlite fall into the "enriched quadrant" and plot intermediate between isotope data for South African "Group I" and "Group II" kimberlites ([32]; Fig. 5A). In contrast, the Hf and Nd isotopic compositions for Somerset Island kimberlites (~100 Ma) emplaced within the Canadian Arctic plot within or proximal to the South African "Group I" kimberlite compositional field [8,11]. Of interest, data for the Diavik kimberlite plot along the oceanic array as defined by Hf–Nd isotopic compositions for oceanic volcanic rocks world-wide [33]. Many South African "Group II" kimberlites and one Somerset Island kimberlite sample also plot along this oceanic array, whereas South African "Group I" kimberlites are displaced below the array (Fig. 5A).

4.4.2. Eclogites

Fourteen eclogites were selected for Hf and Nd isotope analysis (11 low-temperature and 3 high-temperature samples), which represent a large variation in mineral compositions and are characterized by a lack (or minimal evidence) of alteration. The low-temperature eclogites exhibit a significant range in $^{176}Lu/^{177}Hf$ ratios (0.015–0.069). Their corresponding Hf isotopic compositions ($^{176}Hf/^{177}Hf_{(55\ Ma)}$=0.281995–0.284296; $\varepsilon_{Hf(55\ Ma)}$=−26.3 to +55.1) also define a very large variation at the time of kimberlite emplacement 55 Ma ago (Table 2; Fig. 5B), ranging from enriched to highly depleted (compared to a chondritic reservoir). The three high-temperature eclogites are characterized by a much more restricted range in $^{176}Lu/^{177}Hf$ ratios (0.030–0.041) and have Hf isotopic compositions ($^{176}Hf/^{177}Hf_{(55\ Ma)}$=0.283029–0.283137; $\varepsilon_{Hf(55\ Ma)}$=+10.3 to +14.1) that are depleted compared to CHUR at the time of kimberlite emplacement (Table 2; Fig. 5B). $^{147}Sm/^{144}Nd$ ratios (0.042–0.153) and $^{143}Nd/^{144}Nd_{(55\ Ma)}$ ratios (0.510353–0.512793; $\varepsilon_{Nd(55\ Ma)}$) range from −43.2 to +4.4 for the low-temperature eclogites and thus exhibit a large compositional variation (Table 2; Fig. 5B). The high-temperature eclogites are characterized by a more restricted range in $^{147}Sm/^{144}Nd$ ratios (0.118–0.164) and $^{143}Nd/^{144}Nd_{(55\ Ma)}$ ratios (0.512498–0.512643; $\varepsilon_{Nd(55\ Ma)}$ values of −1.4 to +1.5; Table 2; Fig. 5B). Nd and Hf isotope analysis of the diamond–eclogite samples was not possible due to their small sample size.

In an $^{176}Lu/^{177}Hf$ versus $^{176}Hf/^{177}Hf$ isochron diagram, data for the low- and high-temperature eclogites define a relatively well-constrained positively-sloped correlation (Fig. 6A). The regression line calculated based on the Lu–Hf data shown in Fig. 6A corresponds to an 'errorchron age' of 2.1±0.3 Ga (n=14; MSWD=304) with an initial $^{176}Hf/^{177}Hf$ ratio of 0.28170±23 (ε_{Hf} value of +9; Fig. 6A). The Lu–Hf errorchron age is mainly constrained by the data from the low-temperature eclogites since these by themselves also define an identical errorchron age of 2.1±0.3 Ga (initial $^{176}Hf/^{177}Hf$=0.28166±25; MSWD=334; n=11).

4.4.3. Garnet and clinopyroxene

Five garnet–clinopyroxene pairs from the low-temperature eclogites were selected for Hf and Nd isotope analysis. The garnets in the low-temperature eclogites exhibit a large range in $^{176}Lu/^{177}Hf$ ratios (0.043–0.311) and their $^{176}Hf/^{177}Hf_{(55Ma)}$ compositions (0.282925–

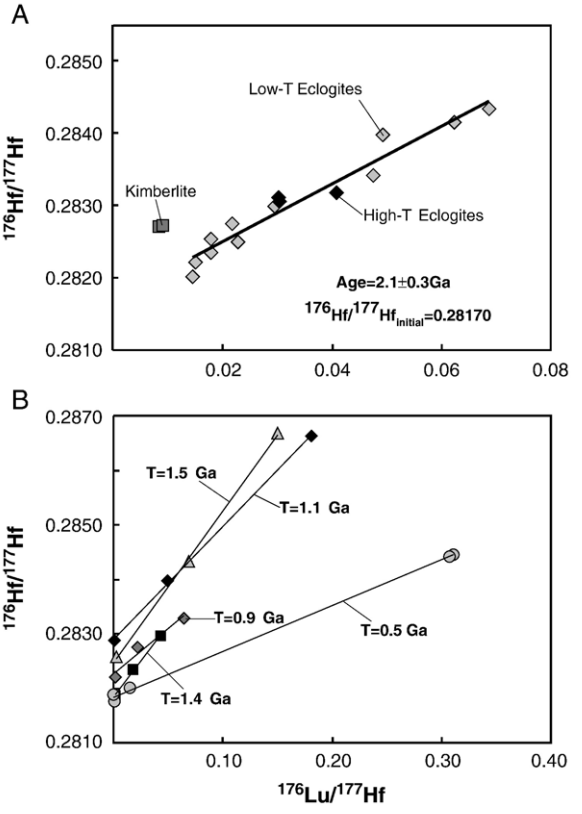

Fig. 6. (A) $^{176}Lu/^{177}Hf$ versus $^{176}Hf/^{177}Hf$ diagram for (A) Diavik eclogites showing 2.1 Ga (billion years) Lu–Hf errorchron and corresponding initial $^{176}Hf/^{177}Hf$ for low-temperature and high-temperature eclogites and (B) Diavik eclogites and their constituent garnets and clinopyroxenes. Tie lines connect constituent minerals with corresponding whole rock composition; one symbol is used for each individual sample. Also shown are the "dates" (in billion years) obtained for individual internal isochrons.

0.286522; $\varepsilon_{Hf(55\ Ma)}$=+6.6 to +133.8) extend to extremely radiogenic values at the time of kimberlite emplacement (Table 2). The clinopyroxenes in the low-temperature eclogites are characterized by very low $^{176}Lu/^{177}Hf$ ratios (0.001–0.003) and less radiogenic $^{176}Hf/^{177}Hf_{(55\ Ma)}$ compositions (0.281768–0.282879; $\varepsilon_{Hf(55\ Ma)}$=−34.3 to +5.0; Table 2) compared to garnets from the same individual samples. Both $^{147}Sm/^{144}Nd$ ratios (0.159–0.702) and $^{143}Nd/^{144}Nd_{(55\ Ma)}$ ratios (0.511030–0.513246; $\varepsilon_{Nd(55\ Ma)}$ values of −30.0 to +13.2; Table 2) for garnets in the low-temperature eclogites exhibit large variations (Table 2). The clinopyroxenes in the low-temperature eclogites have lower $^{147}Sm/^{144}Nd$ ratios (0.031–0.176) and less radiogenic $^{143}Nd/^{144}Nd_{(55\ Ma)}$ ratios (0.510055–0.512763; $\varepsilon_{Nd(55\ Ma)}$ values of −49.0 to +3.8; Table 2) compared to their corresponding garnets.

In an $^{176}Lu/^{177}Hf$ versus $^{176}Hf/^{177}Hf$ isochron diagram, tie lines for garnet–clinopyroxene–whole rock associations from individual samples of low-temperature eclogites are all positively sloped and correspond to internal isochron ages ranging from 0.5 to 1.5 Ga (Fig. 6B). Of importance, correlation coefficients (R^2) for all internal isochrons range from 1.0 to 0.95, suggesting that whole rock eclogites and constituent mineral phases are at isotopic equilibrium. Internal Sm–Nd isochrons for the same garnet–clinopyroxene–whole rock associations yield slightly more variable ages (between 0.1 to 1.4 Ga — not shown; Table 2).

4.5. In-situ Sr and Pb isotope data

In-situ $^{87}Sr/^{86}Sr$ isotope ratios were obtained by laser ablation-MC-ICP-MS for clinopyroxenes from six low-temperature, three high-temperature, and four diamond–eclogites. The range in Sr isotopic values for clinopyroxenes from both low-($^{87}Sr/^{86}Sr$=0.7020–0.7043) and high-temperature eclogites ($^{87}Sr/^{86}Sr$=0.7021–0.7040) are identical (Table 3; Fig. 7), and are all depleted compared to the present-day composition of bulk Earth ($^{87}Sr/^{86}Sr$=0.7045). Most diamond–eclogite clinopyroxenes are characterized by unradiogenic $^{87}Sr/^{86}Sr$ values varying between 0.7027 and 0.7034 with the exception of one sample having slightly more radiogenic $^{87}Sr/^{86}Sr$ values (18088E1; 0.7052–0.7057; Table 3, Fig. 7). The elevated Sr isotopic ratios for sample 18088E1 are attributed to its higher degree of alteration compared to the other clinopyroxenes.

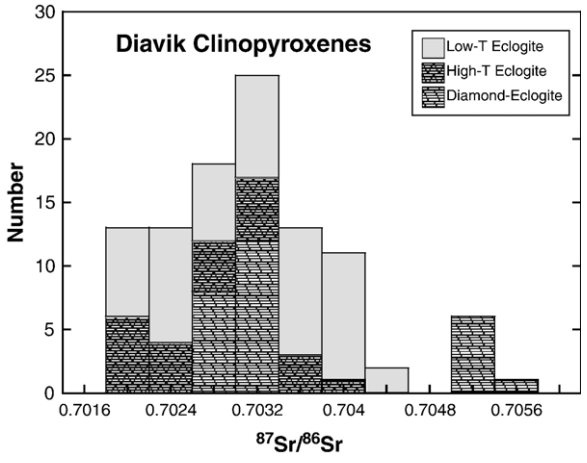

Fig. 7. In-situ $^{87}Sr/^{86}Sr$ isotope ratios obtained by individual laser ablation-MC-ICP-MS analyses for Diavik clinopyroxenes from low-temperature and high-temperature eclogites and diamond–eclogites.

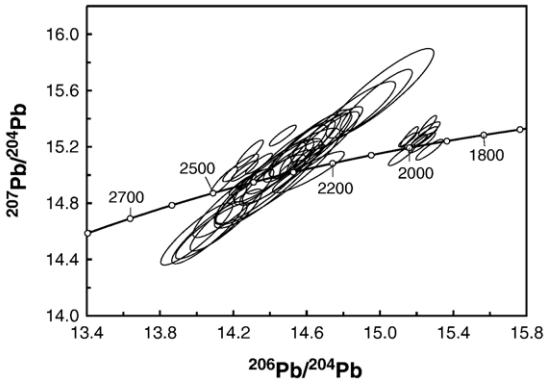

Fig. 8. In-situ Pb isotopic compositions by laser ablation-MC-ICP-MS analyses for clinopyroxenes from three Diavik eclogites. For comparison Stacey–Kramer's [34] evolution of terrestrial Pb is shown.

In-situ Pb isotopic compositions were obtained for clinopyroxenes from three low-temperature (MX2, MX7, MX9; 836–871 °C) Diavik eclogites since only these samples contained sufficient abundances of Pb to allow for laser ablation-MC-ICP-MS analysis. The clinopyroxenes are characterized by extremely unradiogenic Pb compositions ($^{206}Pb/^{204}Pb$=14.47–15.27, $^{206}Pb/^{204}Pb$=15.08–15.58, $^{206}Pb/^{204}Pb$=34.46–36.42; Table 4, Fig. 8). In a Pb–Pb diagram, the clinopyroxene data intersect Stacey–Kramers' [34] evolution curve for terrestrial Pb at ages between 2.4 to 2.3 Ga and 2.0 Ga, respectively (Fig. 8).

5. Discussion

5.1. Kimberlite mantle source

The Diavik kimberlite samples are characterized by essentially chondritic initial $^{176}Hf/^{177}Hf_{(55\ Ma)}$ ratios ($\varepsilon_{Hf(55\ Ma)}$ of −1.1 and −0.8; Table 2; Fig. 5A), while having slightly subchondritic $^{143}Nd/^{144}Nd_{(55\ Ma)}$ ratios (ε_{Nd}

$_{(55\ Ma)}$ of −3.2; Table 2; Fig. 5A). In an Nd–Hf variation diagram, initial isotope ratios for the Diavik kimberlite plot within the "enriched quadrant" (Fig. 5A). Hf isotopic ratios for the Diavik kimberlite overlap the range observed for South African "Group I" kimberlites, whereas their Nd isotope data plot between the compositional fields for South African "Group I" and "Group II" kimberlites ([32]; Fig. 5A). Importantly, the Diavik kimberlite isotopic data fall on the oceanic array encompassing Hf–Nd isotopic data for terrestrial oceanic volcanics [33]. The mantle source for the Diavik kimberlites is characterized by chondritic Hf isotopic ratios while Nd isotope compositions are slightly enriched compared to a chondrite uniform reservoir. These results therefore indicate that the Diavik kimberlites cannot originate from a depleted source such as asthenospheric mantle. It appears likely that the Diavik kimberlites represent melts generated from either continental lithospheric mantle, or a mix of lithospheric and asthenospheric mantle reservoirs. Alternatively, the kimberlites could have been generated from an asthenospheric source containing an enriched component such as recycled continental material.

5.2. Mantle eclogite — age and origin

The major and trace element and isotopic compositions of eclogite xenoliths provide important information in deciphering the origin of these mantle-derived rocks. Whole rock major and trace element compositions can be modeled based on quantitative mass balance calculations using the modal abundances of constituent minerals (i.e. garnet and clinopyroxene) and their respective major and trace element data. The Diavik eclogites and diamond–eclogites have calculated whole rock major element compositions that display broad similarities to data for mafic cumulates from ophiolites (i.e. olivine-gabbros, gabbronorites, gabbros) that are interpreted to represent ancient oceanic crust (e.g. [35,36]; Fig. 9A). The calculated whole rock incompatible trace element compositions for the Diavik eclogites are characterized by low HREE abundances and exhibit flat, parallel patterns in an MORB-normalized diagram (N-MORB; [37]; Fig. 9B). The LREEs show a spectrum from depleted to slightly enriched compositions compared to those for normal MORB (Fig. 9B). All Diavik eclogites are characterized by low abundances of highly incompatible trace elements (e.g. Rb, Ba, Fig. 9B). Most importantly, the Diavik eclogites exhibit both positive Sr and Eu anomalies (Eu/Eu* = 1.1–2.0), with the exception of one sample (MX3: Eu/Eu* = 1.0). Trace element patterns for mafic cumulates from ophiolite sequences (e.g. [36]) show

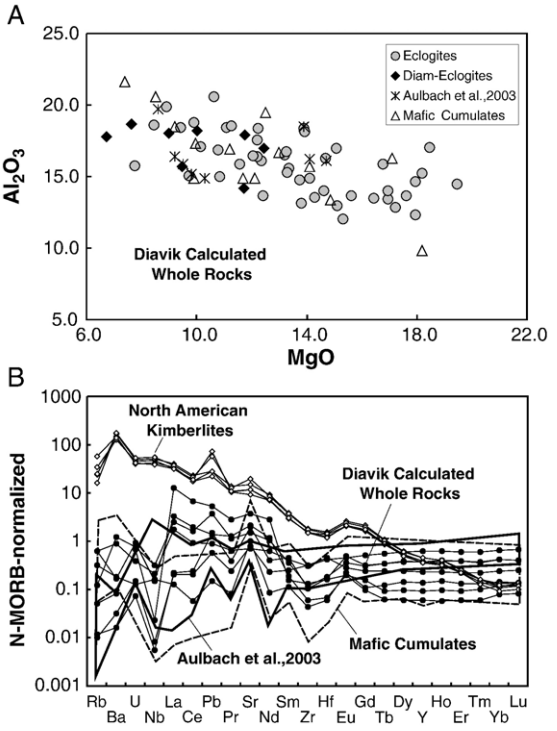

Fig. 9. Calculated whole rock (A) major element compositions for Diavik eclogites and diamond–eclogites and (B) N-MORB-normalized incompatible trace element patterns for Diavik eclogites [37]. Major and trace element data of mafic cumulates from ophiolites representing oceanic crust (dashed line), calculated major and trace element compositions for other Diavik eclogites (solid line) and trace element data for North American kimberlites are shown for comparison [8,35,36,39].

HREE abundances that overlap those for the Diavik eclogites and are characterized by similar positive Sr and Eu anomalies and highly incompatible trace element contents (e.g. Rb., Ba; Fig. 9B). The calculated whole rock LREE contents (e.g. La, Ce) are higher in a few Diavik eclogites (e.g. MX2, MX15; e.g. La, 120 and 600 times chondrite, respectively) compared to those in mafic cumulates from ophiolites, which is mainly a reflection of the high LREE abundances observed in their clinopyroxenes. Clinopyroxene preferentially incorporates LREEs compared to other highly incompatible elements (e.g. Rb, Ba). Thus, the higher whole rock LREE abundances (Fig. 9B) may reflect a recent enrichment event in clinopyroxene resulting from interaction with melts or fluids during mantle metasomatism, and/or interaction with the host kimberlite during sample entrainment. Positive Sr and Eu anomalies have been interpreted as the result of plagioclase accumulation, a feature that is typically observed in cumulate layers within ocean crust sequences (e.g. [38]).

These positive Sr and Eu anomalies and low HREE abundances in combination with xenolith mineralogy are consistent with the interpretation that the protolith for the eclogites and diamond–eclogites from Diavik originates from mafic cumulate phases, such as gabbros, olivine–gabbros and gabbronorites present in oceanic crust rather than normal MORB compositions. Previously reported calculated major and trace element data for eclogites from Diavik are consistent with the results from this study (Fig. 9), and have also been interpreted to represent transformed remnants of mafic oceanic crust [39]. The fact that all Diavik eclogites studied here represent mafic cumulates and not normal MORB compositions may simply be an artifact of sampling bias, since only a small portion of kimberlite has been mined to-date.

The Lu–Hf isotope compositions of the Diavik eclogites plot on an errorchron that yields an age of ~2.1 Ga (Fig. 6A), indicating that formation of the protolith for these rocks occurred in the Paleoproterozoic. Although the Lu–Hf errorchron is constrained predominantly by data for the low-temperature eclogites, the isotopic compositions for all three high-temperature eclogites also fall on the same linear array. This feature may be fortuitous, or indicates that the high-temperature eclogites in fact share the same formational age as the low-temperature eclogites despite their differences in temperature of last equilibration in the lithosphere. The Lu–Hf errorchron yields an initial Hf isotope value that corresponds to an ε_{Hf} value of +9. This result suggests that the Diavik eclogites were derived from a mantle having melt-depleted characteristics rather than a primitive or enriched mantle reservoir. The initial ε_{Hf} value of +9 obtained from the Lu–Hf errorchron corresponds to the Hf isotopic composition of "depleted mantle" at 2.1 Ga [40]. These findings suggest that the Diavik eclogites were derived from a protolith with depleted mantle isotopic characteristics at 2.1 Ga in the Paleoproterozoic. This is consistent with interpretations based on the major element chemistry of the Diavik eclogites (i.e. Fig. 9A).

Contrary to the Lu–Hf isotope results (Fig. 6A), the Sm–Nd isotope systematics for the Diavik eclogites do not define an array in an isochron diagram (not shown; Table 2). This suggests that the initial Nd isotope values of the eclogites may have been subsequently perturbed as the result of isotopic exchange with melts or fluids during mantle metasomatism. This is consistent with the relatively high calculated whole rock LREE (such as Nd) abundances in several eclogite samples (Fig. 4B). In addition, the xenoliths could have suffered contamination with small amounts of host kimberlite magma just prior to or during sample transport, which could have further altered their Nd isotopic composition. These results are in good agreement with findings from many previous studies of mantle xenoliths indicating that Nd isotope systematics are susceptible to isotope exchange during mantle metasomatism, or interaction with the host kimberlite (e.g. [11,41,42]. The Lu–Hf chronometer, in contrast, has demonstrated its capacity of preserving the geological history of mantle xenoliths to a much greater extent, such as recorded in peridotites (e.g. [11,42]) and eclogites in this study.

Internal Lu–Hf isochrons using individual garnet–clinopyroxene–whole rock associations (Fig. 6B) for the low-temperature eclogites yield "ages" ranging from 1.5 to 0.5 Ga. In comparison, internal Sm–Nd isochrons for the same garnet–clinopyroxene–whole rock associations systematically yield slightly younger "ages" varying between 1.4 and 0.1 Ga (Table 2), with the youngest "date" approaching the age of kimberlite emplacement (55 Ma). These results are consistent with the recent findings based on mineral–whole rock Hf isotopic data for cratonic peridotites and high-grade metamorphic rocks suggesting that the closure temperature of the Lu–Hf system is greater than or equal to that of the Sm–Nd system [11,42,43]. However, there is an absence of a garnet–clinopyroxene–whole rock association that defines an internal isochron corresponding to the 2.1 Ga Paleoproterozoic age based on the eclogite whole rock errorchron (Fig. 6A). The complex relationship between diffusion and in-situ radiogenic growth in mantle minerals has been demonstrated in previous studies, indicating that an internal isochron 'age' cannot readily be linked to a specific event (e.g. [44]). Ages post-dating rock formation most likely are the result of partial closure and/or re-equilibration during residence in the lithosphere or during the eruption event (e.g. [45]).

In-situ Sr isotopic compositions for individual Diavik clinopyroxene samples are unradiogenic compared to the composition of present-day bulk Earth. In addition, $^{87}Sr/^{86}Sr$ values overlap between low- and high-temperature eclogites despite their distinct temperatures of last equilibration (Table 3). Of interest, almost all of the diamond–eclogites (except sample 18088E1 that is severely altered) are characterized by $^{87}Sr/^{86}Sr$ values that overlap the range for the eclogites. The Sr isotopic values for the low- and high-temperature eclogites and diamond–eclogites are consistent with derivation from a mantle reservoir having melt-depleted characteristics. This finding corroborates the interpretations based on the depleted mantle Hf isotope characteristics for the Diavik eclogites. The Sr isotopic compositions for

clinopyroxene from both the eclogites and diamond–eclogites strongly support the interpretation that these samples were derived from ancient subducted oceanic crust since mid-ocean ridge basalts were characterized by $^{87}Sr/^{86}Sr$ values of ~0.7020 at 2.1 Ga; [46]. The latter value coincides with the most unradiogenic Sr isotopic values measured for the eclogitic clinopyroxenes (MX9; MX114; Table 3; Fig. 7). In-situ Sr isotopic compositions also correlate with Sr abundances obtained by laser-ablation ICP-MS analysis on the same clinopyroxene grains from individual samples (Fig. 10). Increasing Sr isotopic ratios define two distinct trends, one towards decreasing and the other towards increasing Sr contents. This suggests the involvement of two additional reservoirs having distinct Sr isotopic signatures. Paleoproterozoic seawater was characterized by a $^{87}Sr/^{86}Sr$ value of ~0.7040 at 2.1 Ga [47,48]. Interaction between seawater and oceanic crust has been well documented in previous studies (e.g. [49]) and will result in increasing the $^{87}Sr/^{86}Sr$ of the oceanic protolith (~0.7020). Assuming that the protolith of the Diavik eclogites had inherently variable Sr contents, seawater alteration could explain the trend towards higher Sr isotopic values with decreasing Sr contents (Fig. 10). In contrast, the trend towards increasing Sr isotopic values correlated with higher Sr abundances requires mixing between oceanic crust and a different endmember, such as an incompatible trace element enriched melt or fluid. It appears possible that this endmember is the host kimberlite melt since North American kimberlites are characterized by more radiogenic Sr isotopic compositions and high Sr abundances compared to the Diavik eclogites (e.g. [8,50,51]; Fig. 10). Elevated $^{87}Sr/^{86}Sr$ combined with increasing Sr contents observed in a number of Diavik clinopyroxenes (MX2, MX3, MX7, MX15) could thus be the result of interaction with the host kimberlite just prior to or during sample entrainment (Fig. 10). In addition, the same clinopyroxenes (MX2, MX3, MX7, MX15) are characterized by high LREE abundances (e.g. La, 60–600 times chondrite; Table 1; Fig. 4B) most likely indicating a metasomatic enrichment in these elements. This finding is in good agreement with Sr results for the same samples also suggesting that metasomatic mantle melts or fluids, possibly the host kimberlite, interacted with these eclogites.

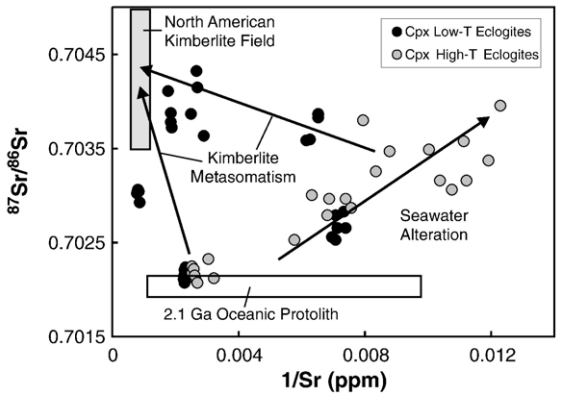

Fig. 10. In-situ $^{87}Sr/^{86}Sr$ isotope ratios versus Sr abundances obtained by laser ablation-analyses for individual Diavik clinopyroxenes from low-temperature and high-temperature eclogites. Data for North American kimberlites are shown for comparison [8,50,51].

The clinopyroxenes from three low-temperature Diavik eclogites (MX2, MX7, MX9; 836–871 °C) are characterized by extremely unradiogenic Pb isotopic compositions ($^{206}Pb/^{204}Pb = 14.47–15.27$; Table 4, Fig. 8). The in-situ clinopyroxene isotopic data intersect the Stacey–Kramers' [34] evolution curve for terrestrial Pb at ages between 2.4 to 2.3 Ga and 2.0 Ga in a Pb–Pb diagram (Fig. 8). These ages are essentially within error of the age obtained from the whole rock Lu–Hf errorchron and thus also support the interpretation that the eclogites formed in the Paleoproterozoic. Of importance, the clinopyroxene Pb isotope data for individual samples indicate significantly older ages than those obtained from corresponding internal Lu–Hf (1.5–1.1 Ga) and Sm–Nd isochrons (1.4–0.4 Ga). These findings suggest that at lithospheric temperatures of 800–900 °C, diffusion of Pb in clinopyroxene appears to be slower than that of Lu–Hf and Sm–Nd in garnet–clinopyroxene assemblages. Preservation of the older Pb isotope ages is consistent with experimental studies on Pb diffusion in clinopyroxene, which indicate that this mineral is capable of retaining its inherited Pb isotopic composition over millions of years when subjected to high temperature conditions within the upper subcontinental lithosphere (800–900 °C; [52]).

5.3. Tectonic evolution of the Slave lithosphere

Geophysical studies have shown that several seismic reflectors exist in the mantle beneath the Slave craton [53,54] strongly indicative of paleosubduction surfaces residing in the subcontinental lithosphere. Therefore, the interpretations presented here based on major and trace element chemistry and Lu–Hf and Sr isotopic systematics of the Diavik eclogites, i.e. the latter represent vestiges of metamorphosed oceanic crust that was subducted beneath the Archean Slave craton, are consistent with the seismic profiling results of the Slave lithosphere. Paleoproterozoic subduction and subsequent accretion of the 1.95–1.91 Ga Hottah terrane

(continental magmatic arc) to the western margin Slave craton during the Wopmay orogeny has been well documented (e.g. [54–56]). East-dipping subduction of oceanic mafic volcanics at the western margin of the Slave craton is also evidenced by the Great Bear magmatic arc that developed after the collision of the Hottah terrane and the Slave craton at ~1.9 Ga (e.g. [57]). It is plausible that the formation of the Diavik eclogites may have been associated with subduction occurring at or prior to 1.95–1.91 Ga, generating the Hottah magmatic arc at the western margin of the Slave craton. The Lu–Hf isotope systematics for the Diavik eclogites presented here are in good agreement with a tectonic model linking their origin to Paleoproterozoic subduction. Formation of oceanic crust most probably occurred ~100 Ma prior to calc-alkaline volcanism related to the Hottah arc. This difference in age appears plausible since the generation of oceanic crust predates its subduction, and this is followed by its transformation into eclogite and associated arc magmatism. These results corroborate the ~2.1 Ga Lu–Hf model ages recorded by mantle zircons from eclogites sampled by the Jericho kimberlite, northwestern Slave Province [12]. The Jericho eclogites have also been interpreted as representing remnants of ancient oceanic lithosphere that was subducted beneath the western margin of the Slave craton in the Paleoproterozoic, based on their isotopic and geochemical characteristics [12,14]. Of interest, a major 2.1 Ga crustal growth event associated with subduction has also been reported for the Birimian Massif (West Africa; [58]). Despite the similarities in age, the kinship of these two tectono-magmatic events on a global scale remains to be evaluated.

The high-temperature eclogites and diamond–eclogites systematically indicate greater depths of last equilibration in the lithosphere compared to the low-temperature eclogites. Of interest, mineral chemical data, calculated whole rock major and trace element compositions and Lu–Hf and Sr isotope systematics for low-and high-temperature eclogites and diamond–eclogites overlap, and thus suggest that all samples were generated by similar rock forming processes. It is possible that the low-temperature eclogites and the high-temperature and diamond–eclogites were formed during subduction of oceanic crust beneath the Slave craton in two separate events. In this case both subduction events must not have occurred more than several millions of years (<100 Ma?) apart, since the oceanic protolith of all Diavik samples was characterized by similar Sr and Hf isotopic compositions and trace elements systematics. Another possibility is that the low-temperature eclogites were formed during subduction related to the Hottah arc magmatism, while the generation of the high-temperature and diamond–eclogites was associated with subduction related to the Great Bear arc magmatism. Alternatively, all eclogites could stem from the same subduction event suggesting that temperature estimates for the eclogites could have been reset during the thermal event associated with kimberlite magmatism; or that a number of samples were transported to shallower depths for a certain period of time prior to their entrainment to the Earth's surface thus allowing them to re-equilibrate at lower ambient temperatures.

6. Conclusions

The eclogites and diamond–eclogites from Diavik are characterized by similar mineral and calculated whole rock major and trace element compositions and isotope systematics strongly suggesting that the same rock forming processes were involved in their generation. Major and trace element data for eclogites and diamond–eclogites are identical to those for mafic cumulates from ophiolite sequences indicative of an oceanic protolith for the Diavik samples. Eclogites and diamond–eclogites are characterized by Hf and in-situ Sr isotope compositions consistent with their derivation from a depleted mantle reservoir, and this supports the interpretation that the eclogites represent fragments of metamorphosed oceanic crust that was subducted beneath the Archean Slave craton. Lu–Hf and in-situ Pb isotope systematics of the Diavik eclogites indicate that formation of their precursor oceanic rocks occurred in the Paleoproterozoic. Plate tectonic reconstruction models for the Slave craton support the findings based on the Hf–Pb–Sr isotope data for the Diavik eclogites, which confirms the existence of subduction regimes adjacent to the Slave craton in the Paleoproterozoic.

Acknowledgments

Funding for this study was provided by Alberta Ingenuity Fund through a postdoctoral fellowship to S. Schmidberger and an NSERC Collaborative Research and Development Grant with Diavik Mines Inc. The Radiogenic Isotope Facility at the University of Alberta is supported, in part, by an NSERC Major Facilities Access Grant.

Appendix A. Supplementary data

Supplementary data associated with this article can be found, in the online version, at doi:10.1016/j.epsl.2006.11.020.

References

[1] I.D. MacGregor, W.I. Manton, Roberts Victor eclogites: ancient oceanic crust, J. Geophys. Res. 91 (1986) 14063–14079.

[2] D.E. Jacob, Nature and origin of eclogite xenoliths from kimberlites, Lithos 77 (2004) 295–316.

[3] R.M. Davies, W.L. Griffin, N.J. Pearson, A.S. Andrew, B.J. Doyle, S.Y. O'Reilly, Diamonds from the deep; Pipe DO-27, Slave Craton, Canada, 7th International Kimberlite Conference Proc., 1999, pp. 148–155.

[4] M.J. O'Hara, H.S. Yoder, Formation and fractionation of basic magmas at high pressure, Scott. J. Geol. 3 (1967) 67–117.

[5] H. Helmstaedt, R. Doig, Eclogite nodules from kimberlite pipes of the Colorado plateau — samples of subducted Franciscan-type oceanic lithosphere, Phys. Chem. Earth 9 (1975) 95–111.

[6] M. Barth, R.L. Rudnick, I. Horn, W.F. McDonough, M.J. Spicuzza, J.W. Valley, S.E. Haggerty, Geochemistry of xenolithic eclogites from West Africa, part 2: origins of the high MgO eclogites, Geochim. Cosmochim. Acta 66 (2002) 4325–4345.

[7] D.G. Pearson, S.B. Shirey, R.W. Carlson, F.R. Boyd, N.P. Pokhilenko, N. Shimizu, Re–Os, Sm–Nd, and Rb–Sr isotope evidence for thick Archean lithospheric mantle beneath the Siberian craton modified by multistage metasomatism, Geochim. Cosmochim. Acta 59 (1995) 959–977.

[8] S.S. Schmidberger, A. Simonetti, D. Francis, Sr–Nd–Pb isotope systematics of mantle xenoliths from Somerset Island kimberlites: evidence for lithosphere stratification beneath Arctic Canada, Geochim. Cosmochim. Acta 65 (2001) 4243–4255.

[9] A.J. Erlank, F.G. Waters, C.J. Hawkesworth, S.E. Haggerty, H.L. Allsopp, R.S. Rickard, M.A. Menzies, Evidence for mantle metasomatism in peridotite nodules from the Kimberley pipes, South Africa, in: M.A. Menzies, C.J. Hawkesworth (Eds.), Mantle Metasomatism, Academic Press, London, 1987, pp. 221–311.

[10] M.A. Menzies, Archean, proterozoic, and phanerozoic lithospheres, in: M.A. Menzies (Ed.), Continental Mantle, Oxford University Press, Oxford, 1990, pp. 67–86.

[11] S.S. Schmidberger, A. Simonetti, D. Francis, C. Gariépy, Probing archean lithosphere using the Lu–Hf isotope systematics of peridotite xenoliths from Somerset Island kimberlites, Canada, Earth Planet. Sci. Lett. 197 (2002) 245–259.

[12] S.S. Schmidberger, L.M. Heaman, A. Simonetti, R.A. Creaser, H.O. Cookenboo, Formation of Paleoproterozoic eclogitic mantle, Slave Province (Canada): insights from in-situ Hf and U–Pb isotopic analyses of mantle zircons, Earth Planet. Sci. Lett. 240 (2005) 621–633.

[13] M.G. Kopylova, J.K. Russell, H. Cookenboo, Mapping the lithosphere beneath the North central Slave craton, 7th International Kimberlite Conference Proc., 1999, pp. 468–479.

[14] L.M. Heaman, R.A. Creaser, H.O. Cookenboo, Extreme enrichment of high field strength elements in Jericho eclogite xenoliths: a cryptic record of Paleoproterozoic subduction, partial melting, and metasomatism beneath the Slave craton, Canada, Geology 30 (2002) 507–510.

[15] W.A. Padgham, The slave structural province, North America: a discussion of tectonic models, in: J.E. Glover, S.E. Ho (Eds.), Third International Archean Symposium Proc. 22, 1992, pp. 381–394.

[16] C. Isachsen, S.A. Bowring, Evolution of the Slave craton, Geology 22 (1994) 917–920.

[17] W. Bleeker, W.J. Davis, The 1991–1996 NATMAP Slave Province project: introduction, Can. J. Earth Sci. 36 (1999) 1033–1042.

[18] W.J. Davis, A.G. Jones, W. Bleeker, H. Grütter, Lithosphere development in the Slave craton: a linked crustal and mantle perspective, Lithos 71 (2003) 575–589.

[19] H.O. Cookenboo, Extension of ultradepleted mantle within the Contwoyto Terrane of the Slave craton, northern Canada, 8th International Kimberlite Conference Abstr., 2003.

[20] M. Bizzarro, J.A. Baker, D. Ulfbeck, A new digestion and chemical separation technique for rapid and highly reproducible determination of Lu/Hf and Hf isotope ratios in geological materials by MC-ICP-MS, Geostand. Newsl. 27 (2003) 133–145.

[21] R.A. Creaser, L.M. Heaman, P. Erdmer, Timing of high-pressure metamorphism in the Yukon–Tanana terrane, Canadian Cordillera: constraints from U–Pb zircon dating of eclogite from the Teslin tectonic zone, Can. J. Earth Sci. 34 (1997) 709–715.

[22] S.S. Schmidberger, A. Simonetti, D. Francis, Small-scale Sr isotope investigation from peridotite xenoliths by laser ablation MC-ICP-MS — implications for mantle metasomatism, Chem. Geol. 199 (2003) 317–329.

[23] A. Simonetti, L.M. Heaman, R.P. Hartlaub, R.A. Creaser, T.G. MacHattie, C. Böhm, U–Pb zircon dating by laser ablation-MC-ICP-MS using a new multiple ion counting Faraday collector array, J. Anal. At. Spectrom. 20 (2005) 677–686.

[24] B.L. Gulson, Uranium–lead and lead–lead investigations of minerals from the Broken Hill lodes and mine sequence rocks, Econ. Geol. 79 (1984) 476–490.

[25] D. Canil, D.J Schulze, D. Hall, B.C. Hearn Jr., S.M. Milliken, Lithospheric roots beneath western Laurentia: the geochemical signal in mantle garnets, Can. J. Earth Sci. 40 (2003) 1027–1051.

[26] N.J. Pearson, W.L. Griffin, B.J. Doyle, S.Y. O'Reilly, E. van Achterbergh, K. Kivi, Xenoliths from kimberlites pipes of the Lac de Gras area, Slave craton, Canada, 7th International Kimberlite Conference Proc., 1999, pp. 644–658.

[27] E.J. Krogh, The garnet–clinopyroxene Fe–Mg geothermometer — a reinterpretation of existing experimental data, Contrib. Mineral. Petrol. 99 (1988) 44–48.

[28] W.F. McDonough, S.S. Sun, The composition of the earth, Chem. Geol. 120 (1995) 223–253.

[29] J. Blichert-Toft, F. Albarède, The Lu–Hf isotope geochemistry of chondrites and the evolution of the mantle–crust system, Earth Planet. Sci. Lett. 148 (1997) 243–258.

[30] J.B. Dawson, A review of the geology of kimberlite, in: P.J. Wyllie (Ed.), Ultramafic and Related Rocks, Wiley, New York, 1967, pp. 241–251.

[31] C.B Smith, Pb, Sr and Nd isotopic evidence for sources of southern African Cretaceous kimberlites, Nature 304 (1983) 51–54.

[32] G.M. Nowell, D.G. Pearson, D.R. Bell, R.W. Carlson, C.B. Smith, P.D. Kempton, S.R. Noble, Hf isotope systematics of kimberlites and their megacrysts: new constraints on their source regions, J. Petrol. 45 (2004) 1583–1612.

[33] J.D. Vervoort, P.J. Patchett, J. Blichert-Toft, F. Albarède, Relationships between Lu–Hf and Sm–Nd isotopic systems in the global sedimentary system, Earth Planet. Sci. Lett. 168 (1999) 79–99.

[34] J.S. Stacey, J.D. Kramers, Approximation of terrestrial lead isotope evolution by a two-stage model, Earth Planet. Sci. Lett. 26 (1975) 207–221.

[35] U. Bağci, O. Parlak, V. Höck, Whole rock and mineral chemistry of cumulates from the Kizildağ (Hatay) ophiolite (Turkey): clues for multiple magma generation during crustal accretion in the southern Neotethyan ocean, Mineral. Mag. 69 (2005) 53–76.

[36] M. Benoit, M. Polvé, G. Ceuleneer, Trace element and isotopic characterization of mafic cumulates in a fossil mantle diaper (Oman ophiolite), Chem. Geol. 134 (1996) 199–214.

[37] A.W. Hofmann, Chemical differentiation of the Earth: the relationship between mantle, continental crust, and oceanic crust, Earth Planet. Sci. Lett. 90 (1988) 297–314.
[38] B. Hamelin, B. Lambret, J.-L. Joron, M. Treuil, C.J. Allègre, Geochemistry of basalts from the Tyrrhenian Sea, Nature 278 (1979) 832–834.
[39] S. Aulbach, W.L. Griffin, N.J. Pearson, S.Y. O'Reilly, K. Kivi, B.J. Doyle, Origins of eclogites beneath the central Slave craton, 8th International Kimberlite Conference Abstr., 2003.
[40] P.J. Patchett, O. Kouvo, C.E. Hedge, M. Tatsumoto, Evolution of continental crust and mantle heterogeneity: evidence from Hf isotopes, Contrib. Mineral. Petrol. 78 (1981) 279–297.
[41] D.G. Pearson, The age of continental roots, Lithos 48 (1999) 171–194.
[42] R.-M. Bedini, J. Blichert-Toft, M. Boyet, F. Albarède, Isotopic constraints on the cooling of the continental lithosphere, Earth Planet. Sci. Lett. 223 (2004) 99–111.
[43] E.E. Scherer, K.L. Cameron, J. Blichert-Toft, Lu–Hf garnet geochronology: closure temperature relative to the Sm–Nd system and the effects of trace mineral inclusions, Geochim. Cosmochim. Acta 64 (2000) 3413–3432.
[44] A. Zindler, E. Jagoutz, Mantle cryptology, Geochim. Cosmochim. Acta 52 (1988) 319–333.
[45] M. Gunther, E. Jagoutz, The meaning of Sm/Nd apparent ages from kimberlite-derived coarse grained low temperature peridotites from Yakutia, Russ. Geol. Geophys. 38 (1997) 229–239.
[46] M. Rehkamper, A.W. Hofmann, Recycled oceanic crust and sediment in Indian Ocean MORB, Earth Planet. Sci. Lett. 147 (1997) 93–106.
[47] J. Veizer, W. Compston, $^{87}Sr/^{86}Sr$ in Precambrian carbonates as an index of crustal evolution, Geochim. Cosmochim. Acta 40 (1976) 905–914.
[48] J. Veizer, W. Compston, N. Clauer, M. Schidlowski, $^{87}Sr/^{86}Sr$ in late Proterozoic carbonates: evidence for a "mantle" event at ~900 Ma ago, Geochim. Cosmochim. Acta 47 (1983) 295–302.
[49] A. Zindler, H. Staudigel, S.R. Hart, R. Endres, S. Goldstein, An in-depth Nd and Sr isotope study of a mafic layer from the Ronda ultramafic complex, Nature 304 (1983) 226–230.
[50] L.M. Heaman, The nature of the subcontinental mantle from Sr–Nd–Pb isotopic studies on kimberlite perovskite, Earth Planet. Sci. Lett. 92 (1989) 323–334.
[51] D.P. Dowall, D.G. Pearson, G.M. Nowell, B.A. Kjarsgaard, J. Armstrong, M.S.A. Horstwood, Comparative geochemistry of kimberlites from the Lac de Gras field, NWT — an integrated isotopic and elemental study, 8th International Kimberlite Conference Abstr., 2003.
[52] D.J. Cherniak, Pb diffusion in Cr diopside, augite, and enstatite, and consideration of the dependence of cation diffusion in pyroxene on oxygen fugacity, Chem. Geol. 177 (2001) 381–397.
[53] M.G. Bostock, Anisotropic upper-mantle stratigraphy and architecture of the Slave craton, Nature 390 (1997) 392–395.
[54] F.A. Cook, A.J. van der Velden, K.W. Hall, Frozen subduction in Canada's Northwest Territories: lithoprobe deep lithospheric reflection profiling of the western Canadian Shield, Tectonics 18 (1999) 1–24.
[55] P.F. Hoffman, Wopmay orogen: a Wilson cycle of early Proterozoic age in the northwest of the Canadian Shield, in: D.W. Strangway (Ed.), The Continental Crust and its Mineral Deposits, Geol. Assoc. Can. Spec. Pap., vol. 20, 1989, pp. 523–549.
[56] E.M. Moores, R.J. Twiss, Tectonics, W.H Freeman, New York, 1995, p. 415.
[57] R.S. Hildebrand, P.F. Hoffman, S. Bowring, Tectono-magmatic evolution of the 1.9 Ga Great Bear magmatic zone, Wopmay orogen, northwestern Canada, J. Volcanol. Geotherm. Res. 32 (1980) 99–118.
[58] M. Boher, W. Abouchami, A. Michard, F. Albarède, N.T. Arndt, Crustal growth in West Africa at 2.1 Ga, J. Geophys. Res. 97 (1992) 345–369.